The Central Kiloparsec of Starbursts and AGN: The La Palma Connection
ASP Conference Series, Vol. 249, 2001
J. H. Knapen, J. E. Beckman, I. Shlosman, and T. J. Mahoney, eds.

2001ASPC..249..187S

A Near-Infrared Imaging Survey of Nearby Spiral Galaxies

S. Stedman[1], J. H. Knapen[1,2], and D. M. Bramich[2]

[1]*University of Hertfordshire, Dept of Physical Sciences, Hatfield, Herts. AL10 9AB, UK*

[2]*Isaac Newton Group of Telescopes, Apartado 321, E-38700 Santa Cruz de La Palma, Spain*

Abstract. *K*-band imaging was carried out on a sample of 57 spiral galaxies to map their stellar backbones, examine the underlying mass distribution across the arm and interarm regions, and perform bulge:disk decomposition. As within the broader aims of the project, which also use *B*, *I*, and Hα images, our results will be examined in the light of global parameters including Hubble stage, Elmegreen arm class, and quantity and distribution of recent massive star formation and dust.

1. Introduction

Near-infrared (NIR) imaging of galaxies in the *K* band is a good tracer of the stellar populations in the massive disk due to the reduced extinction by dust and the low contribution of emission from young stars at these wavelengths. NIR images show both axisymmetric and non-axisymmetric features in the surface brightness distribution, which make up the stellar backbone of the galaxy (e.g., Rix 1993; Rix & Zaritsky 1995; Regan & Elmegreen 1997). Evidence of any density-wave enhancement in the mass will be visible from the arm:interarm mass-enhancement ratio. Other enhancements in mass and light such as inner rings, resonances, and underlying bars will also be visible at this wavelength (Elmegreen et al. 1999; Pérez-Ramírez et al. 2000).

This information will be used as part of our main project in which we are studying global and arm versus interarm star formation (SF) rates and properties in spiral galaxies using *B*, *I*, *K*, and Hα data. In previous work on a handful of galaxies (Knapen & Beckman 1996; Beckman et al. 1996; Grøsbol & Patsis 1998) the interarm radial behavior of the exponential disk was found to be similar to that of the complete disk, but that of the arms alone was strikingly different. The increase in scale-length in the arms was interpreted as being due to the influence of enhanced SF. If confirmed generally, this effect would raise important questions about the complete disk scale-length used in many global studies. Building upon our previous work, we will calculate the scale-lengths of the exponential disks of a sample of spiral galaxies to determine, firstly, the "true" underlying disk scale-length, and, secondly, how this "true" scale-length is influenced by local enhancements in the SF rate.

© Astronomical Society of the Pacific • Provided by the NASA Astrophysics Data System

2001ASPC..249..187S

2. Sample Selection

The sample was extracted from that used by Elmegreen & Elmegreen (1987), who list approximately 580 galaxies from the *Second Reference Catalogue of Bright Galaxies* (de Vaucouleurs et al. 1976). This sample can be considered a statistically complete, representative sample covering a range of morphological types, and whose arm classes (Elmegreen & Elmegreen 1987) range from flocculent to grand design. Details of the sample and selection criteria can be found in Stedman & Knapen (2001).

Table 1. Spiral galaxy sample: NGC number and the Hubble type from de Vaucouleurs et al. 1991

NGC	Type	NGC	Type	NGC	Type	NGC	Type
210	SX3	3227	SX1	4254	SA5	5247	SA4
337A	SX8	3344	SX4	4303	SX4	5248	SX4
488	SA3	3351	SB3	4314	SB1	5334	SB5
628	SA5	3368	SX2	4321	SX4	5371	SX4
864	SX5	3486	SX5	4395	SA9	5457	SX6
1042	SX6	3631	SA5	4450	SA2	5474	SA6
1068	SA3	3726	SX5	4487	SX6	5850	SB3
1073	SB5	3810	SA5	4535	SX5	5921	SB4
1169	SX3	4030	SA4	4548	SB3	5964	SB7
1179	SX6	4051	SX4	4579	SX3	6140	SB6
1300	SB4	4123	SB5	4618	SB9	6384	SX4
2775	SA2	4145	SX7	4689	SA4	6946	SX6
2805	SX7	4151	SX2	4725	SX2	7727	SX1
2985	SA2	4242	SX8	4736	SA2	7741	SB6
3184	SX6						

3. Observations and Results

The observations were made with the INGRID camera on the William Herschel Telescope for all galaxies except four. The INGRID camera uses a 1024 $\times$ 1024 HgCdTe HAWAII array, optimized for imaging between 0.8 to 2.5 μm. The scale is 0.242″ per pixel, giving a 4.13′ $\times$ 4.13′ field of view. The K_s filter (central wavelength 2.150 μm) was used for these observations, and mosaics were made of the larger galaxies.

Using the IRAF ELLIPSE task, radial ellipses were fitted around a fixed central position, giving radial profiles of position angle (P.A.) and ellipticity (ϵ), as shown for NGC 4254 in Figure 1. The runs of P.A. and ϵ were then used to fix the ellipse-fitting parameters at each point of major changes across the disk. The ELLIPSE task was repeated to give an azimuthally averaged isophotal analysis of the galaxy (Beckman et al. 1996; Seigar & James 1998).

© Astronomical Society of the Pacific • Provided by the NASA Astrophysics Data System

2001ASPC..249..187S

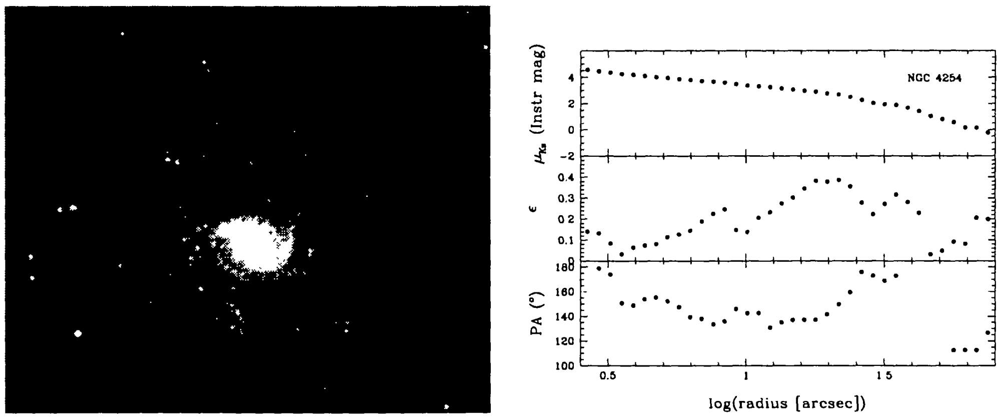

Figure 1. NGC 4254 is a Hubble type Sc galaxy with an Elmegreen classification of 9, denoting two symmetric inner arms with multiple long and continuous outer arms (*left*). The image measures 4.13 arcmin × 4.13 arcmin; E is to the *left* and N is *up*. Surface brightness, ellipticity, and position-angle radial profiles of the complete disk (*right*).

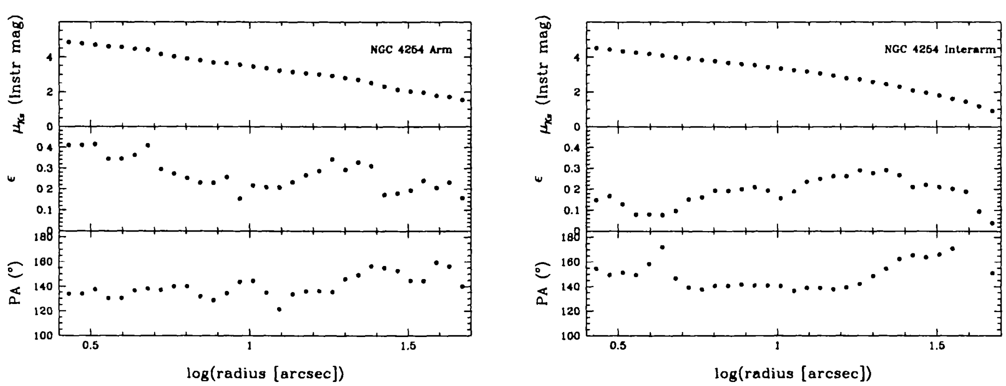

Figure 2. As Fig. 1, now for the arm regions only (*left*) and interarm only (*right*).

© Astronomical Society of the Pacific • Provided by the NASA Astrophysics Data System

2001ASPC..249..187S

To determine the underlying mass distribution across the arm and interarm regions, the galaxies were normalized to enhance the appearance of fainter structures such as weak spiral arms. Normalization was carried out by constructing a model of the smooth axisymmetric bulge and disk component from the isophotal brightness profile, and dividing this into the original galaxy image. Masks were constructed to separate the arm and interarm regions for detailed radial-profile analysis of these regions, as shown in Figure 2. The masks create a map of the underlying mass distribution, which will be used in future work to reveal the possible presence of density waves. The technique of normalizing the galaxy further highlights any faint structures not otherwise visible (Beckman et al. 1996), and this will be used to examine the circumnuclear structure of the entire sample.

4. Conclusions

Our multiband imaging of a carefully selected sample of 57 spiral galaxies of all types will allow us to study the influence of SF on the exponential scale-lengths of the disks and to correct the measured all-disk scale-lengths for SF effects.

Acknowledgments. We thank Dr. R. S. de Jong for providing us with K_s images of four of our sample galaxies. The William Herschel Telescope is operated on the island of La Palma by the Isaac Newton Group in the Spanish Observatorio del Roque de los Muchachos of the Instituto de Astrofísica de Canarias.

References

Beckman, J. E., Peletier, R. F., Knapen, J. H., Corradi, R. L. M., & Gentet, L. J. 1996, ApJ, 467, 175

de Vaucouleurs, G., de Vaucouleurs, A., & Corwin, H. G., Jr. 1976, Second Reference Catalogue of Bright Galaxies (Austin: Univ. Texas Press)

de Vaucouleurs, G., de Vaucouleurs, A., Corwin, H. G., Buta, R. J., Paturel, G., & Fouqué, P. 1991, Third Reference Catalogue of Bright Galaxies (New York: Springer)

Elmegreen, D. M., & Elmegreen, B. G. 1987, ApJ, 314, 3

Elmegreen, D. M, Chromey, F. R., Sawyer, J. E., & Reinfeld, E. L. 1999, AJ, 118, 777

Grøsbol, P. J., & Patsis, P. A. 1998, A&A, 336, 840

Knapen, J. H., & Beckman, J. E. 1996,MNRAS, 283, 251

Pérez-Ramírez, D., Knapen, J. H., Peletier, R. F., Laine, S., Doyon, R., & Nadeau, D. 2000, MNRAS, 317, 234

Regan, M. W., & Elmegreen, D. M. 1997, AJ, 114, 965

Rix, H.-W. 1993, PASP, 105, 999

Rix, H.-W., & Zaritsky, D. 1995, ApJ, 447, 82

Seigar, M. S., & James, P. A. 1998, MNRAS, 299, 685

Stedman, S., & Knapen, J. H. 2001, Ap&SS, in press

© Astronomical Society of the Pacific • Provided by the NASA Astrophysics Data System

2001ASPC..249..187S

Part 3

The Physical Properties of AGN

© Astronomical Society of the Pacific • Provided by the NASA Astrophysics Data System